

A new approach for determining accurate chemical distributions using *in-situ* GCIB cross-section imaging

Shin-ichi Iida,^{a*} Takuya Miyayama,^b Gregory L. Fisher,^b John S. Hammond,^b Scott R. Bryan^b and Noriaki Sanada^a

Time-of-flight secondary ion mass spectrometry (TOF-SIMS) has become widely used to characterize various kinds of materials, especially organic materials. It has recently become possible to investigate the molecular distributions underneath the surface using Ar-GCIB (gas cluster ion beam) depth profiling. It is an important new capability for practical use of TOF-SIMS because the subsurface and interface chemistry plays an important role in the performance of many products. However, it is difficult to obtain accurate chemical depth distributions using sputter depth profiling when the sample has a significant surface roughness and/or inhomogeneous structure. In order to resolve this problem, we proposed an approach to determine the accurate chemical distributions using GCIB cross-section imaging method. In this study, this approach was demonstrated for practical organic samples, and accurate chemical depth distributions were determined. Copyright © 2014 John Wiley & Sons, Ltd.

Keywords: organic depth profiling; accurate chemical distributions; *in-situ* GCIB cross-section imaging

Introduction

Time-of-flight secondary ion mass spectrometry (TOF-SIMS) is a powerful tool to determine the distribution of chemical species at the outermost surface with high sensitivity, high spatial resolution, and high mass resolution. These features make TOF-SIMS advantageous for the analysis of organic materials. The function of organic materials is rapidly progressing, and in many cases, the structure is becoming more complicated. Therefore, it has become important to investigate the molecular distributions on and underneath the surface in order to relate the chemical and molecular structure to the material performance. To probe the molecular depth gradients of organic materials, Ar gas cluster ion beam (Ar-GCIB) depth profiling has been applied.^[1–3] However, sputter depth profiling has some limitations. Several reports showed that it was difficult to obtain accurate chemical and molecular distributions, when samples had an initial surface roughness, inhomogeneous structures, or significant crater bottom roughness resulting from the depth profiling.^[4,5] To solve the problems, accurate chemical depth scale information is thought to be required, especially for engineered organic devices and materials. We have already reported on *in-situ* Ga focused ion beam (FIB) sample cross-sectioning and liquid metal ion gun (LMIG) observation.^[6] The study showed that more accurate depth scale was obtained by TOF-SIMS analysis of *in-situ* cross-sectioned sample. In the present study, we proposed an approach using *in-situ* Ar-GCIB sample cross-sectioning followed by imaging the cross-section with a LMIG, and applied this method to practical organic samples. The results showed that the accurate chemical distributions could be determined over a depth of 10–100 μm with a high mass resolution.

Experimental

The sputter depth profiling, *in-situ* cross-sectioning, and imaging were performed using a commercial TOF-SIMS instrument (TRIFT V nanoTOF, ULVAC-PHI Inc.) equipped with an Ar gas cluster ion gun, LMIG, and TRIFT mass spectrometer.^[7] For sputter depth profiling and cross-sectioning, an Ar_{2500}^+ ion beam at 20 keV was used, and the typical current of the Ar-GCIB was 15 nA. For LMIG imaging, a primary ion beam of 60 keV Au_3^{++} ions were used and 2D images were reconstructed from the mass intensity in the pixel. The 10 eV electrons were irradiated for charge compensation during sputtering and TOF-SIMS measurements. The incident angles of the Au_3^{++} and Ar_{2500}^+ ions were 40° from the sample normal. The samples analyzed for the experiment were commercial adhesive tape with 46 μm in the thickness attached on a polyethylene terephthalate (PET) film, and commercial polyethylene-nylon 6-6 wrap film 10 μm in thickness. Sputtered depths were measured with a mechanical stylus profiler (Dektak 6 M, Veeco). The trajectory of secondary ions ejected from the cross-section was simulated by computer software (SIMION 8.0, Scientific Instrument Services Inc.). X-ray photoelectron spectroscopy (XPS) analysis was performed using a commercial XPS instrument (PHI 5000 VersaProbe, ULVAC-PHI, Inc.) equipped with an Ar gas cluster ion gun and a monochromated Al K α scanning X-ray source.

* Correspondence to: Shin-ichi Iida, ULVAC-PHI Inc., 370 Enzo Chigasaki Kanagawa, 253-8522, Japan.
E-mail: shinichi_iida@ulvac.com

^a ULVAC-PHI Inc., 370 Enzo, Chigasaki, Kanagawa, 253-8522, Japan

^b Physical Electronics Inc., 18725 Lake Drive East, Chanhassen, MN, 55317, USA

The scheme of GCIB cross-section imaging was shown in Fig. 1. The organic sample surface was covered by a metal mask prior to loading it into the TOF-SIMS instrument to avoid any crater formation or irregular irradiation damage on the surface area of the organic samples. In the present study, we used 50- μm thick titanium sheet as the metal mask. Other metals with low sputter rates compared with that of organic materials were also possible to produce the cross-section. The masked sample was introduced to the analysis chamber, and then, Ar-GCIB was irradiated onto the edge of the metal mask. After preparation of the cross-section, TOF-SIMS images were acquired with the pulsed LMIG. The depth resolutions for the cross-section imaging and sputter depth profiling were defined as the distance between 16–84% intensity change at the interface.

Results and discussion

SIMION simulation

Our previous study showed that ejection angle (α) between the secondary ions and the optical axis of the analyzer should be set typically less than 10° in order to detect the secondary ions.^[8] To support this, and find the optimal condition to detect the secondary ions from the whole area of the cross-section, we simulated the secondary ion trajectory using the model calculation. Figure 2 shows the simulation result of secondary ion trajectory from the cross-section surface, assuming the sample was electrically conducting. Sample thickness used for the simulation was 100 μm . Extraction field gradient was 1.5×10^6 V/m. This result also showed that the secondary ion trajectory was drawn perpendicular to the potential contour line. It was confirmed that tilt angle of the stage should be 10° to optimize secondary ion detection from the whole cross-section area.

GCIB cross-section

The sputter rates of Ar-GCIB on organic materials are typically very high (up to 1 $\mu\text{m}/\text{min}$), whereas the sputter rates on metals are extremely low. As expected, the cross-section of the samples was prepared quickly, and total ion dose to create a cross-section of 46- μm thick adhesion tape and 10- μm thick wrap film was approximately 9×10^{16} ions/ cm^2 (cross-sectioning time: 1600 sec) and $\sim 6 \times 10^{16}$ ions/ cm^2 (cross-sectioning time: 600 s), respectively. There was no trace of crater observed on the titanium plate even after cross-sectioning to a dose that was 10 \times (approximately 10^{18} ions/ cm^2) higher than the condition required for the polymer milling.

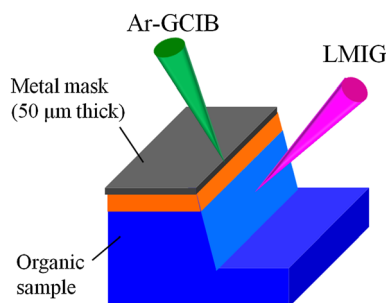


Figure 1. Schematic illustration of the gas cluster ion beam cross-section imaging method.

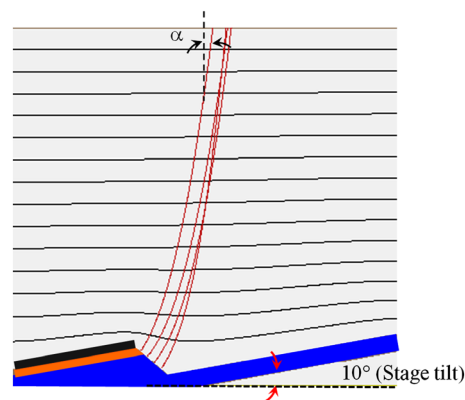


Figure 2. Simulation results of electric field (black line) and secondary ion trajectory (red line) around the cross-sectioned sample surface with a tilting angle of 10° . Alpha (α) in the figure represents the ejection angle with respect to the axis of the input lens.

Adhesion tape

The adhesion tape used in the experiment has polypropylene (PP) and acrylic adhesive layers.^[9] Figure 3 showed the negative ion spectra of each layer. After the cross-sectioning, TOF-SIMS images were acquired. The primary ion dose was maintained within the static limit (1.7×10^{12} ions/ cm^2). As shown in Fig. 4 (a), PP, acrylic adhesive, and PET layers were clearly observed. A strip of unsputtered top surface was also observed because the mask created a shadow from the GCIB, which has a 40° incident angle. From the results, we confirmed that high mass resolution over 5000 ($M/\Delta M$) was obtained, and it was possible to collect secondary ions without significant loss of the signal (Fig. 4(b)–(d)). In addition to the mass images, the mass spectrum of PET region was also shown in Fig. 4(e), which suggested the present technique could be employed with higher mass-to-charge ratio ions. Figure 5 showed the intensity profiles of $\text{C}_3\text{H}_3\text{O}_2^-$ and $\text{C}_7\text{H}_5\text{O}_2^-$ from those images. The depth resolutions at the PP/acrylic adhesive and acrylic adhesive/PET interfaces were 450 and 600 nm, respectively. The results suggested that the depth scale less than 1 μm could be obtained. Total thickness of the adhesion tape was 46 μm , thus

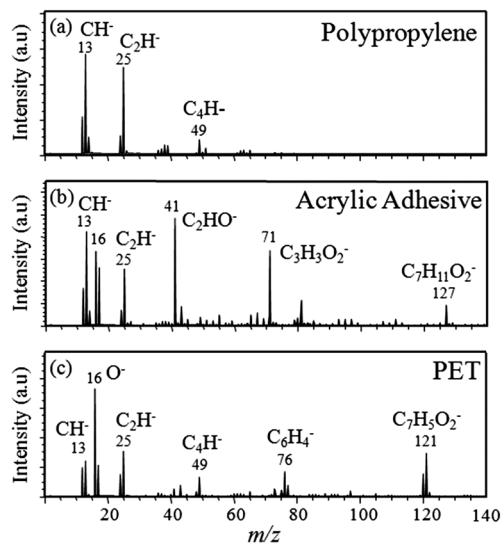


Figure 3. Negative ion spectra of (a) polypropylene; (b) acrylic adhesive; and (c) polyethylene terephthalate.

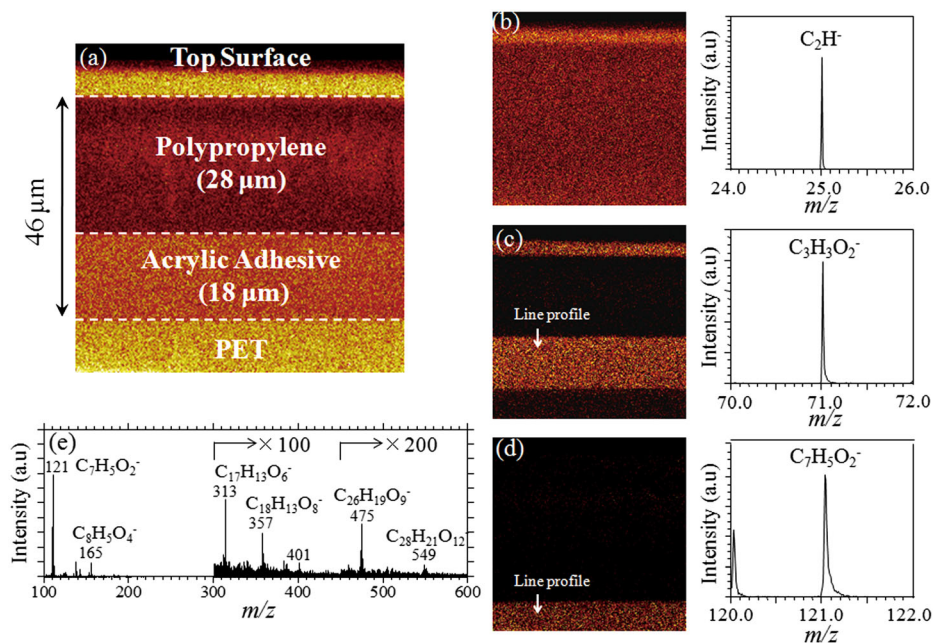


Figure 4. Cross-section images of adhesion tape on polyethylene terephthalate (PET). (a) Total ion; (b) C_2H^- ; (c) $C_3H_3O_2^-$; and (d) $C_7H_5O_2^-$ images. The mass spectrum extracted from PET region was shown in (e). Enlarged secondary ion mass peaks of C_2H^- , $C_3H_3O_2^-$, and $C_7H_5O_2^-$ extracted at each image were also shown. The arrows in (c) and (d) indicate the distances that the depth resolutions were determined from the intensity profile in Fig. 5.

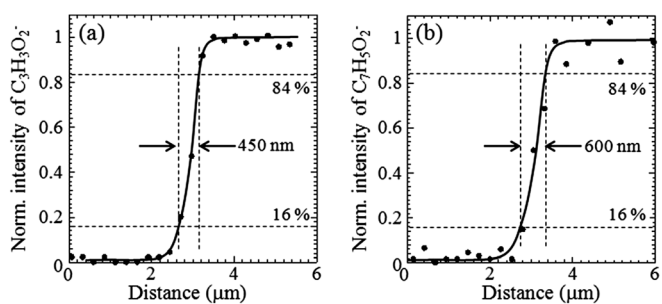


Figure 5. Intensity profiles of (a) $C_3H_3O_2^-$ and (b) $C_7H_5O_2^-$ at the polypropylene/acrylic adhesive and acrylic adhesive/polyethylene terephthalate interfaces.

the thickness of PP and acrylic adhesive layers were 28 and 18 μm , by measuring the ratio of each layer width. Figure 6(a) showed the result of sputter depth profiling. The XPS and/or TOF-SIMS Ar-GCIB depth profiling provided us the ultrahigh depth resolution ($<10\text{ nm}$);^[10] however, it was not easy to convert the sputter time into depth scale when the sample had inhomogeneous structures. From the cross-section image and measurement of the total crater

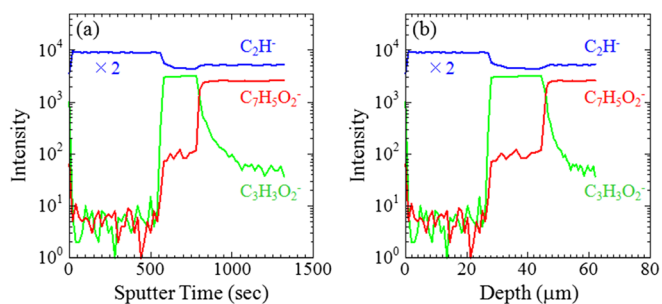


Figure 6. Changes of the secondary ion intensities (a) with respect to the sputter time; (b) after conversion into the depth scale.

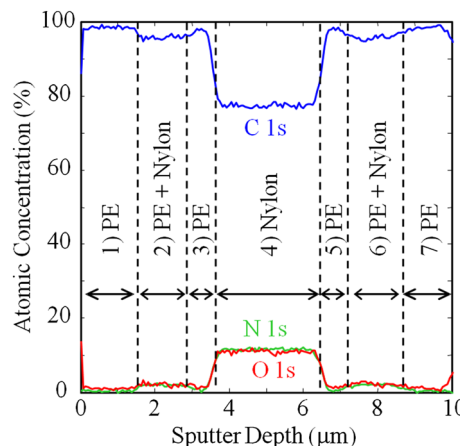


Figure 7. Result of Ar gas cluster ion beam depth profiling of wrap film using X-ray photoelectron spectroscopy.

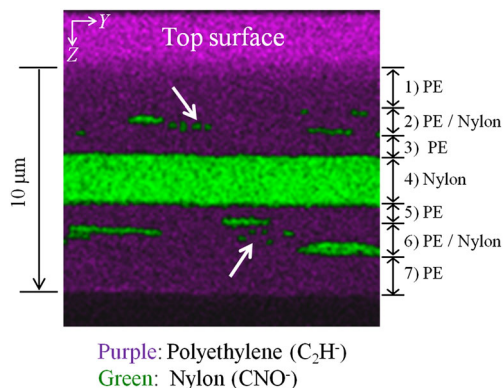


Figure 8. Overlaid mass image of the cross-section of a wrap film. The cross-section was cut *in-situ* with Ar gas cluster ion beam ion sputtering with titanium metal mask within 10 minutes.

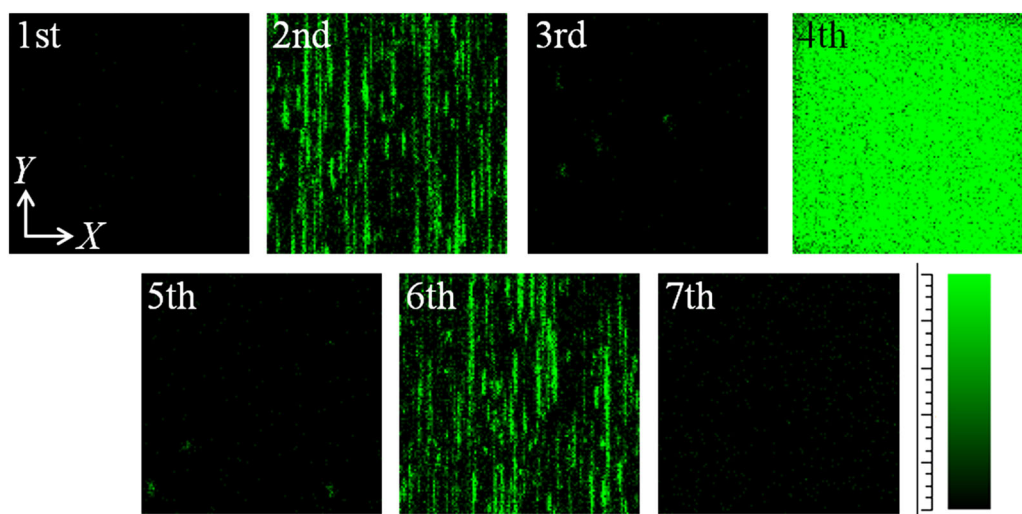


Figure 9. Change in 2D mass images of CNO^- ion taken by sputter depth profiling. Ordinal number 1–7 stand for the layers of the sample. The field of view of the images is $50\ \mu\text{m} \times 50\ \mu\text{m}$.

depth after the depth profiling ($62\ \mu\text{m}$), it is possible to convert the sputter time into the depth scale (Fig. 6(b)). In sputter depth profile, the depth resolution at acrylic adhesive/PET interface was worse than that at PP/acrylic adhesive interface (1500 and 650 nm, respectively), suggesting that the resolution would become worse as a function of the depth because of the mixing and/or surface roughening. On the other hand, the depth resolutions of the cross-section imaging at both interfaces were similar with each other (600 and 450 nm). Those results indicated that the present method would have an advantage for the determination of chemical depth distributions of thicker organic samples.

Wrap film

The organic layer structure was analyzed by using combination of XPS and Ar-GCIB sputtering. As shown in Fig. 7, the presence of seven organic layers was observed. Figure 8 showed the cross-section TOF-SIMS image overlay of the wrap film. The purple and green colors showed the polyethylene (C_2H^-) and nylon 6-6 (CNO^-) images, respectively. The seven organic layers were also confirmed in the cross-section image. Sub-micron features of nylon were observed in the second and sixth layers (indicated by white arrows). In order to investigate the structure of the film, sputter depth profiling was also performed. Figure 9 showed the change in 2D mass images of CNO^- ion with respect to sputtered depth; the field of view of the image was $50\ \mu\text{m} \times 50\ \mu\text{m}$. The fiber-like nylon structures along Y direction were observed. The sub-micron features observed in Fig. 8 were the cross-cut of the fibers.

Conclusion

In the present study, we proposed and investigated an approach using an *in-situ* Ar-GCIB cross-sectioning and TOF-imaging in order to determine accurate chemical depth distributions. Because of the very large difference in sputter rates of Ar-GCIB on organic materials relative to metals, this method is highly practicable for thick organic materials. This new method enables us to obtain the accurate depth scale, provides high throughput analysis, and would be useful for complicated, highly engineered organic materials in a wide range of industries.

References

- [1] S. Ninomiya, K. Ichiki, H. Yamada, Y. Nakata, T. Seki, T. Aoki, J. Matsuo, *Rapid Commun. Mass Spectrom.* **2009**, *23*, 1601.
- [2] T. Miyayama, N. Sanada, S. R. Bryan, J. S. Hammond, M. Suzuki, *Surf. Interface Anal.* **2010**, *42*, 1453.
- [3] I. Yamada, J. Khoury, in *MRS Proceedings (Vo. 1354 No.1)*, Cambridge University Press, **2011**, doi: 10.1557/opl.2011.1081.
- [4] M. A. Robinson, D. J. Graham, D. G. Castner, *Anal. Chem.* **2012**, *84*, 4880.
- [5] S. Muramoto, J. Brison, D. G. Castner, *Surf. Interface Anal.* **2011**, *43*, 58.
- [6] A. Wucher, G. L. Fisher, C. M. Mahoney, in *Cluster Secondary Ion Mass Spectrometry* (Ed: C. M. Mahoney), John Wiley and Sons, Hoboken, **2013**, pp. 207–246.
- [7] B. W. Schueler, in *TOF-SIMS: Material Analysis by Mass Spectrometry* (2nd edn), (Eds: J. C. Vickerman, D. Briggs), IM Publications, Surface Spectra, Manchester, **2013**, pp. 247–270.
- [8] S. Iida, N. Sanada, *J. Surf. Anal.* **2012**, *18*, A-61.
- [9] Product information, <http://www.mmm.co.jp>. [Last accessed August 20th, 2013].
- [10] A. G. Shard, R. Havelund, M. P. Seah, S. J. Spencer, I. S. Gilmore, N. Winograd, D. Mao, T. Miyayama, E. Niehuis, D. Rading, R. Moellers, *Anal. Chem.* **2012**, *84*, 7865.